VOLUME 113, NUMBER 19
SEPTEMBER 11, 1991

JOURNAL
OF THE
AMERICAN
CHEMICAL
SOCIETY

Structural Analysis of a Camphor-Derived Cyclopentadienyllithium Compound by NMR and MNDO. A Ternary Equilibrium in Tetrahydrofuran[1]

Walter Bauer,*,† George A. O'Doherty,‡ Paul von Ragué Schleyer,† and Leo A. Paquette‡

Contribution from the Institut für Organische Chemie der Universität Erlangen-Nürnberg, Henkestrasse 42, D-8520 Erlangen, Federal Republic of Germany, and Evans Chemical Laboratories, The Ohio State University, Columbus, Ohio 43210. *Received January 7, 1991*

Abstract: At −107 °C, the camphor-derived cyclopentadienyllithium compound **2** (CCpLi) exists as three different aggregates in tetrahydrofuran solution. These are the *exo*-lithio monomer **10**, the *endo*-lithio monomer **11**, and the *endo,endo*-lithio dimer **12**, in a 57:21:22 molar ratio (0.34 M solution). Approximately the same composition of these three species is present at room temperature. The identification was achieved by 1D and 2D NMR methods. Due to ring-current phenomena, unusual upfield ^{6}Li NMR chemical shifts are observed (δ = −7.83 ppm for the two monomers **10** and **11** and −12.45 ppm for "sandwiched" lithium in dimer **12**). MNDO calculations on the individual isomers are in agreement with the experimentally determined relative stabilities. The results rationalize earlier findings concerning the endo stereoselectivity in reactions of **2** with Ti and Zr electrophiles.

Introduction

Lithium isodicyclopentadienide (**1**) (isodiCpLi) and the related camphor derivative **2** (CCpLi) behave quite differently in reactions with electrophiles. Depending on temperature, **1** reacts stereoselectively with methyl iodide to yield the endo product **3** at low temperatures (−78 °C) or the exo product **4** at room temperature (Scheme I).[2a] In analogous reactions with appropriate titanium, zirconium, iron, ruthenium, and osmium electrophiles, the stereochemically related transition-metal species are formed.[2b-d]

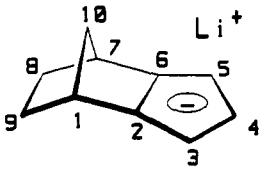

1

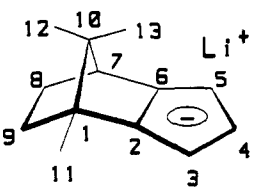

2

Scheme I

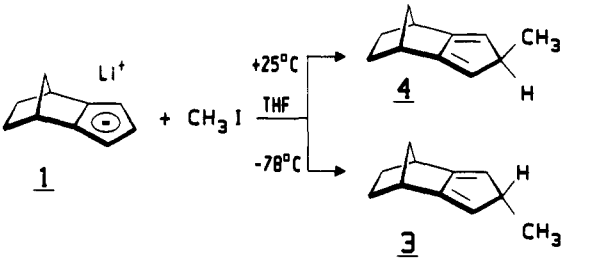

1 **4** **3**

By contrast, metalation of the optically active CCpLi (**2**) with various titanium and zirconium halides proceeds only at room temperature or at elevated temperatures. Irrespective of the

† Institut für Organische Chemie.
‡ Evans Chemical Laboratories.

(1) Isodicyclopentadienes and Related Molecules. 58. Part 57: Rogers, R. D.; Sivik, M. R.; Paquette, L. A. Submitted for publication.
(2) (a) Paquette, L. A.; Charumilind, P.; Kravetz, T. M.; Böhm, M. C.; Gleiter, R. *J. Am. Chem. Soc.* **1983**, *105*, 3126. (b) Paquette, L. A.; Moriarty, K. J.; Meunier, P.; Gautheron, B.; Sornay, C.; Rogers, R. D.; Rheingold, A. L. *Organometallics* **1989**, *8*, 2159. (c) Paquette, L. A.; Moriarty, K. J.; Meunier, P.; Gautheron, B.; Crocq, V. *Ibid.* **1988**, *7*, 1873. (d) Paquette, L. A.; Schirch, P. F. T.; Hathaway, S. J.; Hsu, L.-Y.; Gallucci, J. *Ibid.* **1986**, *5*, 490.

0002-7863/91/1513-7093$02.50/0

solvent and structure of the electrophile, a preference for endo complexation is seen throughout.[3] For example, a 7/1 mixture of diastereomers **5** and **6** is formed when **2** reacts with $CpTiCl_3$ in tetrahydrofuran (THF) at room temperature.

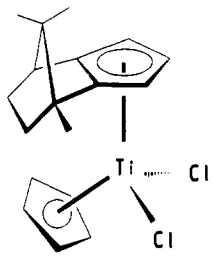

5

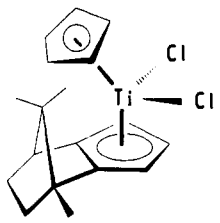

6

Recently, we have studied the structure of isodiCpLi (**1**) in THF solution in detail.[4] At low temperatures (−100 °C), an equilibrium mixture of exo monomer **7** and exo,exo dimer **8** was detected. However, at room temperature exo monomer **7** was the prevailing species.

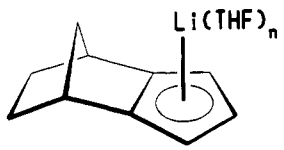

7

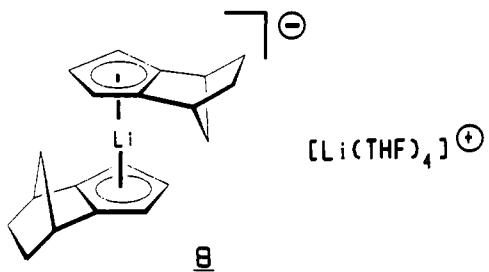

8

In this investigation we present a combined NMR and MNDO investigation of CCpLi (**2**). Although similarities with isodiCpLi (**1**)[4] facilitated the NMR analysis, dynamic phenomena and the occurrence of more than two aggregates complicated the spectral assignments.

Results and Discussion

^{1}H and ^{13}C NMR at Room Temperature. We employed samples of CCpLi (**2**) enriched 96% in the ^{6}Li isotope for the NMR studies. The merits of using ^{6}Li instead of the major naturally abundant ^{7}Li isotope are well-known.[5] The proton and carbon NMR spectra of an ca. 0.3 M solution of **2** in THF-d_8 at +25 °C each show one set of signals. As discussed in detail below, there is rapid interchange (on the NMR time scale) between different aggregates at this temperature. Hence, time-averaged signals are observed.

The spectral assignments were achieved by using standard two-dimensional NMR techniques[6] (^{1}H,^{1}H COSY, ^{1}H,^{13}C shift correlation, COLOC; these spectra are not shown in this paper).

Table I. ^{1}H Chemical Shifts of CCpLi (**2**) at 25 and −107 °C (δ, ppm) in THF-d_8, 0.24 M

		−107 °C		
H	25 °C	**10**	**11**	**12**
3	5.31 (m)	5.25	5.34	4.89
4	5.34 (m)	5.40	5.10	4.72
5	5.34 (m)	5.25	5.34	4.95
7	2.51 (d, 3.6 Hz)	2.60	2.43	2.25
8 (exo)	1.89 (tt, 3.6 Hz, 10.4 Hz)	1.81	*a*	1.85
8 (endo)	0.90 (dt, 3.7 Hz, 10.1 Hz)	0.72	*a*	1.66
9 (exo)	1.67 (dt, 3.7 Hz, 9.9 Hz)	1.55	*a*	1.69
9 (endo)	0.98 (dt, 3.2 Hz, 9.4 Hz)	0.76	*a*	1.69
11	1.16 (s)	1.20	*a*	1.01
12	0.86 (s)	0.89	*a*	0.76
13	0.65 (s)	0.85	0.34	0.14

[a] Not identified unambiguously due to small signal height and/or signal overlap.

Table II. ^{13}C Chemical Shifts of CCpLi (**2**) at 25 and −107 °C (δ, ppm) in THF-d_8, 0.34 M

		−107 °C		
C	25 °C	**10**	**11**	**12**
1	51.67	51.77	*a*	50.86
2	133.34	131.79	133.07	131.96
3	94.51	93.75	*a*	94.25
4	99.09	100.84	95.09	96.88
5	96.01	95.09	*a*	95.54
6	128.75	127.07	128.91	127.37
7	51.96	51.42	*a*	50.76
8	30.41	30.71	30.06	28.92
9	37.82	37.80	37.18	36.06
10	59.55	56.85	64.10	64.02
11	14.05	14.49	*a*	14.67
12	21.18	21.31	*a*	21.45
13	21.53	21.45	*a*	21.45

[a] Not identified unambiguously. No indirect detection via C,H shift correlation could be achieved.

The proton and carbon chemical shifts of **2** at room temperature are listed in Tables I and II.

In the ^{13}C NMR spectrum, the carbon (C11) of one of the three methyl groups resonates appreciably upfield from the other two, C12 and C13. This is also the case in the parent hydrocarbon 9.[7] The less clearcut NMR assignment of CH_3 (C12) and CH_3

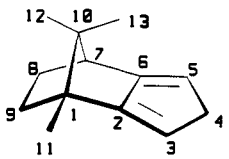

9

(C13) of **2** was achieved by a phase-sensitive NOESY experiment[6] (not depicted);[8] the ^{1}H NMR singlet at 0.86 ppm exhibits cross peaks with the resonances of H8(exo) and H9(exo) due to dipolar interactions. By contrast, analogous cross peaks for the ^{1}H resonance at 0.65 ppm are missing. Consequently, the ^{1}H singlet at highest field (0.65 ppm) is assigned to H13, whereas H12 resonates downfield at 0.86 ppm.

^{1}H and ^{13}C NMR Spectra at Low Temperature. At −107 °C, the ^{1}H and ^{13}C NMR spectra of a 0.34 M solution of **2** in THF-d_8 each show *three* sets of signals (cf. one-dimensional spectra in Figure 1). Due to continuing rapid exchange at the lowest accessible temperature (THF freezes at −108 °C), some of the ^{1}H and ^{13}C signals are broadened considerably. We demonstrate below that the three species observed must be the exo monomer **10**, the endo monomer **11**, and the endo,endo dimer **12**. Under

(3) Paquette, L. A.; Moriarty, K. J.; McKinney, J. A.; Rogers, R. D. *Organometallics* **1989**, *8*, 1707.
(4) Paquette, L. A.; Bauer, W.; Sivik, M. R.; Bühl, M.; Feigel, M.; Schleyer, P. v. R. *J. Am. Chem. Soc.* **1990**, *112*, 8776.
(5) (a) Seebach, D.; Hässig, R.; Gabriel, J. *Helv. Chim. Acta* **1983**, *66*, 308. (b) Fraenkel, G.; Hsu, H.; Su, B. M. In *Lithium. Current Applications in Science, Medicine, and Technology*; Bach, R. O., Ed.; Wiley: New York, 1985. (c) Günther, H.; Moskau, D.; Bast, P.; Schmalz, D. *Angew. Chem.* **1987**, *99*, 1242. *Angew. Chem., Int. Ed. Engl.* **1987**, *26*, 1212.
(6) Kessler, H.; Gehrke, M.; Griesinger, C. *Angew. Chem.* **1988**, *100*, 507. *Angew. Chem., Int. Ed. Engl.* **1988**, *27*, 490.
(7) Vollhardt, P. C.; Halterman, R. L. *Tetrahedron Lett.* **1986**, *27*, 1461.
(8) Neuhaus, D.; Williamson, M. *The Nuclear Overhauser Effect in Structural and Conformational Analysis*; VCH: New York, 1989.

these conditions, the molar ratio is 57:21:22, respectively.

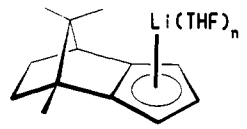

10

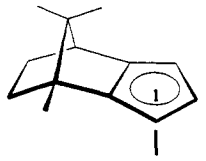

11

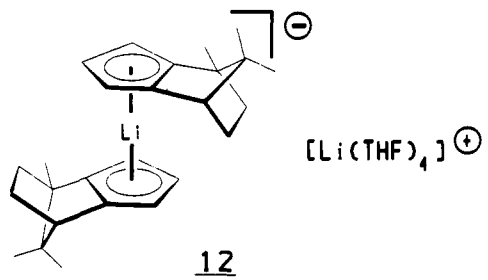

12

A first indication that the major species was the *exo*-lithio monomer **10** came from the more than 7 ppm upfield ^{13}C chemical shift of C10, relative to the analogous resonances in the remaining two species. This agrees with findings for the exo and endo titanium complexes; the ^{13}C chemical shift of the methano-bridge carbon atom of exo compound **13** is 11.4 ppm upfield from the corresponding shift of the endo compound **14**.[2b] Note also the

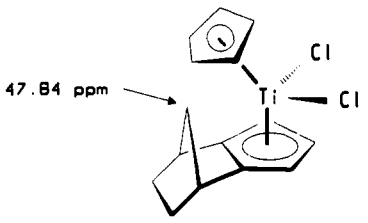

13

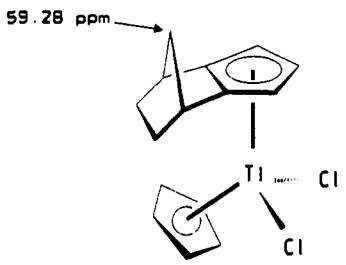

14

similar observations made earlier for the camphor-derived endo,endo and exo,exo titanium complexes **15** and **16**.[3]

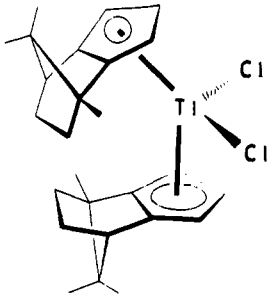

15

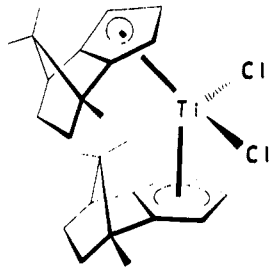

16

Further evidence for exo location of lithium in the major species is based on the chemical shifts of the H8 and H9 protons; the difference for each exo and endo proton pair is ca. 1.1 ppm. This is consistent with results for analogous titanium and zirconium compounds;[2b,3] large ^1H chemical shift differences for the diastereotopic proton pairs at C8 and C9 are found when the metal is positioned exo. In contrast, the corresponding endo isomers of the same species show nearly identical ^1H chemical shifts for the analogous geminal protons. Evidently, close proximity of the cation (Ti, Zr) produces a downfield shift of the endo H8 and H9 hydrogen atoms. In our case, this situation is found in the endo, endo dimer **12** (Figure 1), where the proton resonances of H8 endo,exo and H9 endo,exo lie within a narrow range (1.69–1.85 ppm; cf. Table I). Therefore, lithium must be located at the endo face of the Cp rings in **12**. Endo location of lithium in this isomer is further indicated by the ^{13}C chemical shift, δ, of C10, which is appreciably larger than δ (C10) of exo monomer **10** (Table II).

Independent indications for the lithium location come from the chemical shifts of the syn methyl protons, H13. In the endo,endo dimer **12**, the corresponding signal appears at very high field (δ = 0.14 ppm). Obviously, ring-current effects are responsible; these protons lie in the shielding cones of the Cp rings. By contrast, the corresponding resonance in the exo monomer **10** appears farther downfield (δ = 0.85 ppm). This may be due to agostic interactions between the exo lithium atom and the H13 hydrogen atoms. Lithium generally exerts a deshielding effect on nearby protons.[9] MNDO calculations support this interpretation (see below).

Further evidence for the location of the cation in **10** and **12** is provided by the sequence of chemical shifts for the three Cp protons, H3, H4, and H5. In the major isomer **10**, the order is $\delta_{H4} > \delta_{H3,H5}$ (Table I). This agrees with the sequence found in the analogous exo titanocene compounds **6**[3] and **13**,[2b] as well as in exo isodiCpLi monomer **7** and in exo,exo isodiCpLi dimer **8**.[4] Consequently, lithium has an exo location in the major isomer **10** of Figure 1.

In contrast, this order is reversed in endo,endo dimer **12** ($\delta_{H5} > \delta_{H3} > \delta_{H4}$), consistent with results obtained for the endo titanocene complexes **5**[3] and **14**.[2b] Accordingly, **12** must have endo lithium locations.

In order to confirm the aggregation in the endo,endo dimer **12**, a 2D rotating frame nuclear Overhauser effect spectrum (ROESY)[6,8] was recorded. Like the familiar NOESY experiment,[6,8] ROESY permits the detection of short proton–proton distances. These are indicated by appropriate cross peaks in 2D plots. Moreover, cross peaks due to chemical exchange (which are inherent to both NOESY and ROESY) may be distinguished in ROESY from ROE peaks due to their opposite phases. This is not possible when NOESY is used outside the "extreme narrowing limit" (i.e. at low temperatures); under such conditions exchange and NOE cross peaks appear with identical phases.

We used the same strategy for the identification of the assumed endo,endo dimer **12** as that described for isodiCpLi (**1**).[4] In the hypothetical exo,exo dimer sandwich **17**, the *inter*ligand contact between the Cp protons of one subunit and the protons H13 of the syn methyl group of the opposing ligand should be indicated by appropriate cross peaks in the ROESY spectrum. No close contacts between the Cp protons and more remote H8,H9 endo protons are expected. In contrast, the endo,endo dimer **12** should show close *inter*ligand proton–proton contacts between H3, H4, and H5 of one ligand and H8,H9(endo) of the second ligand, indicated by the appropriate cross signals. No cross peaks due to interligand contacts between H3, H4, and H5 and H13 are expected.

Figure 2a shows a contour plot section of the ROESY spectrum of **2**, which contains cross peaks originating from dipolar interactions. Under the measurement conditions (−107 °C, spin lock time 250 ms), there is still rapid exchange between the different isomers. Thus, cross peaks also appear at "false" positions (those which are not directly involved in the ROE buildup). However,

(9) (a) Bauer, W.; Schleyer, P. v. R. *J. Am. Chem. Soc.* **1989**, *111*, 7191. (b) Bauer, W.; Feigel, M.; Müller, G.; Schleyer, P. v. R. *Ibid.* **1988**, *110*, 6033. (c) Bauer, W.; Winchester, W. R.; Schleyer, P. v. R. *Organometallics* **1987**, *6*, 2371. (d) Bauer, W.; Clark, T.; Schleyer, P. v. R. *J. Am. Chem. Soc.* **1987**, *109*, 970.

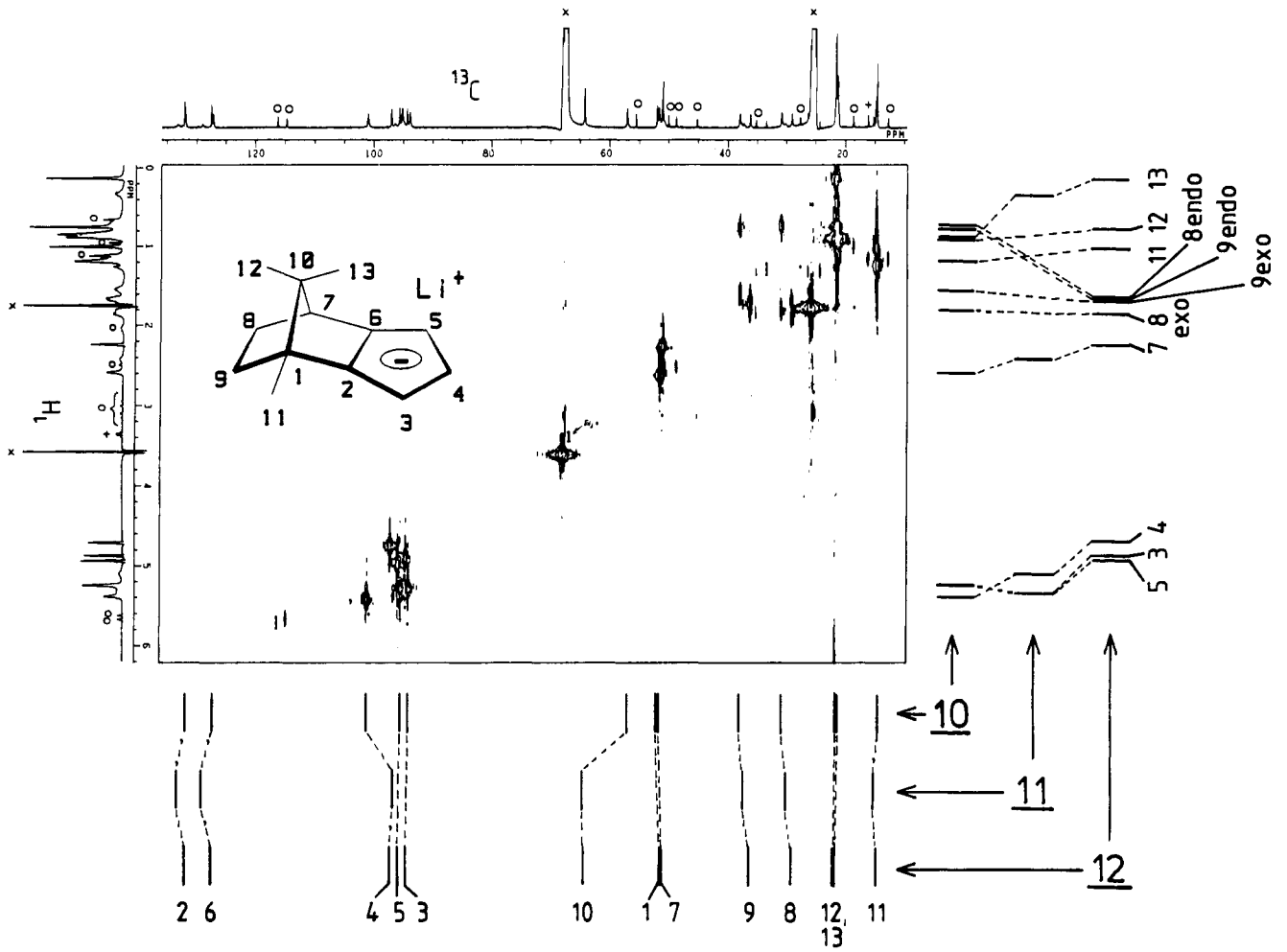

Figure 1. $^1H,^{13}C$ shift correlated 2D NMR spectrum of CCpLi **2**, 0.34 M in THF-d_8 at −107 °C. Peak assignments: × = solvent signal; + = diethyl ether; o = educt **9**. The one-dimensional ^1H spectrum is shown with slight resolution enhancement (Gaussian weighting).

for neither f_1 cross section of H13 for all three observed isomers do any cross peaks appear that involve the "aromatic" protons H3, H4, and H5 (empty boxes in the contour plot). This indicates that neither an exo,exo dimer **17** nor an exo,endo dimer **18** is involved.

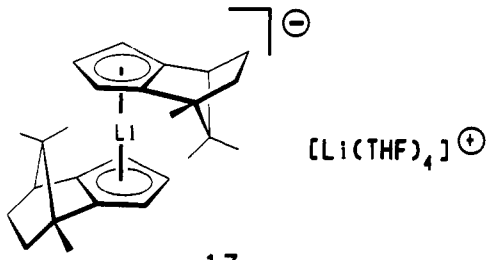

17

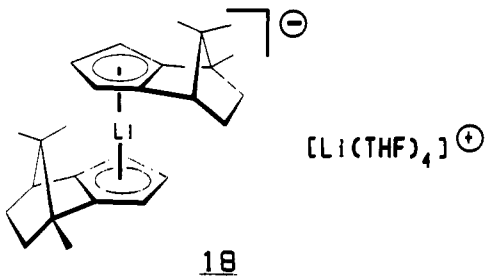

18

Instead, the cross peaks between H3, H4, and H5 and H8 and H9 (endo) expected for the endo,endo dimer **12** appear at the indicated positions (arrows in Figure 2a). In addition, a "false" (transferred) ROE cross peak is visible between H3 and H5 of exo monomer **10** and H8 and H9 of endo,endo dimer **12** (dashed arrow). This must originate from chemical exchange.

Figure 2b shows the "opposite" side of the ROESY contour plot. This contains diagonal peaks as well as cross peaks due to chemical exchange and HOHAHA transfer.[8] The off-diagonal peaks indicate that *three* species are in equilibrium (note the resonances of H7 and H13 of the three species, indicated by arrows in Figure 2b).

Some of the ^1H and ^{13}C resonance lines of the third species (visible in Figures 1 and 2 but not discussed before) are broadened due to exchange/coalescence phenomena even at −107 °C. This third species might be either the exo,exo dimer **17** or the endo monomer **11**. Due to the presence of only one set of signals for this isomer, a mixed exo,endo dimer **18** can be ruled out.

The spectral features described above characterizing **10** and **12** may also be used to identify the endo monomer **11**. The chemical shift of the syn methyl protons, H13, is closer to that of endo,endo dimer **12** than to that of exo monomer **10** (Table 1). This is consistent with the location of these protons in the lithium "unperturbed" shielding cone of the Cp ring.

The ^{13}C chemical shift of C10 of the endo monomer **11** is nearly identical with that of the endo,endo dimer **12**. This is consistent with the "remoteness" of lithium from the methano-bridge carbon atom. The sequence of the Cp ring ^1H chemical shifts of **11** is identical with that found for the endo,endo dimer **12** (δ_{H5}, $\delta_{H3} > \delta_{H4}$). This also helps to confirm the endo location of lithium in **11**.

^{6}Li NMR at −107 °C. Unusual ^{6}Li NMR spectra were observed for isodiCpLi (**1**).[4] As there are two chemically nonequivalent lithium sites in dimer **8**, the equilibrium mixture of exo monomer

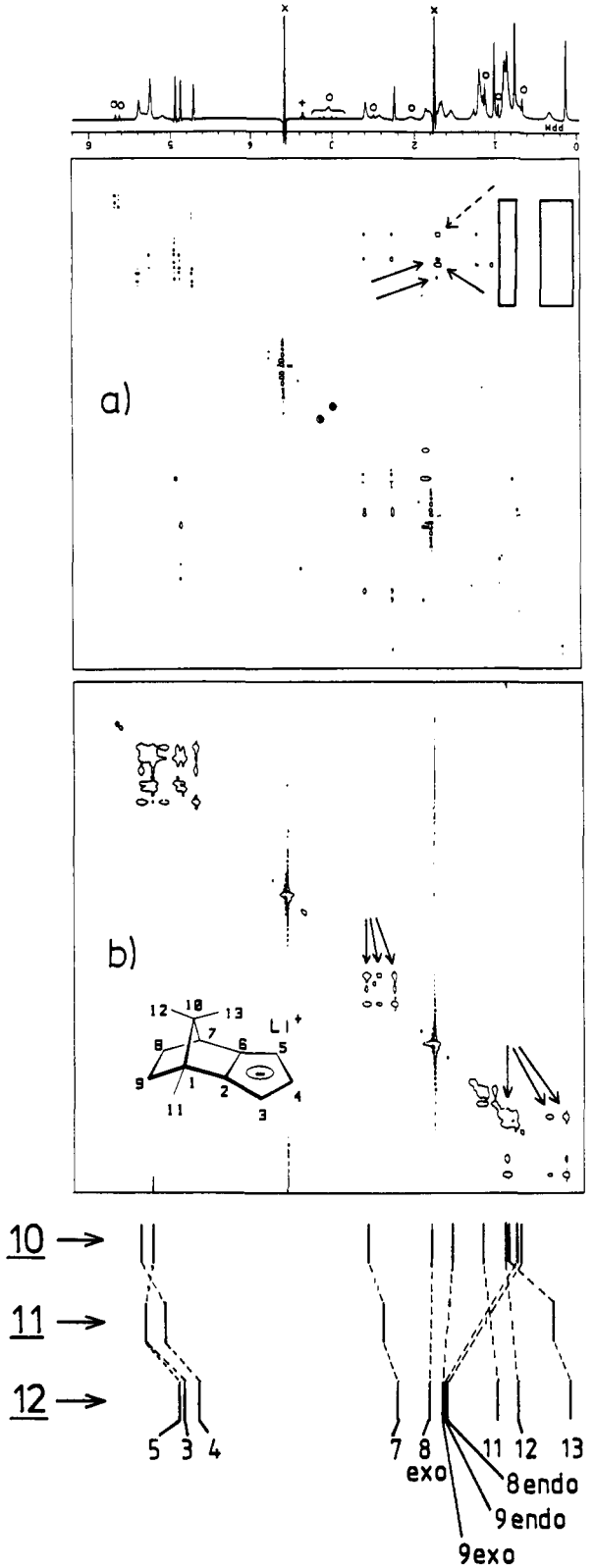

Figure 2. ROESY spectrum of CCpLi **2** in THF-d_8, −107 °C, 0.34 M; spin lock time, 250 ms. (a) Negative contours indicating ROE cross peaks. (b) Positive contours, indicating diagonal, HOHAHA, and exchange cross peaks. For an explanation of the arrows and empty boxes in the contour plots, see text. The ×, +, and ○ peak assignments are as in Figure 1. The one-dimensional spectrum is shown with slight Gaussian resolution enhancement.

7 and exo,exo dimer **8** displays *three* ^{6}Li signals. Due to the location of Li over one Cp ring in **7** and due to "sandwiching" between two Cp rings in **8**, strong upfield shifts are observed: δ = −7.64 ppm for lithium in **7** and δ = −12.78 ppm for the "sandwiched" lithium in **8**. The THF-solvated "external" counterion in **8** resonates in the "normal" range at δ = −1.10 ppm. IGLO calculations on the lithium chemical shifts were in agreement with the experimental results.[4]

The ^{6}Li NMR spectrum of a 0.34 M solution of CCpLi (**2**) at −107 °C is almost identical with that of isodiCpLi (**1**); three signals at δ = −0.98, δ = −7.83, and δ = −12.45 ppm are observed (cf. Figure 3). Without prior knowledge, one might assign these *three* signals to the *three* isomers detected by ^{1}H and ^{13}C NMR. However, this interpretation is not correct. Rather, the ^{6}Li chemical shifts of the exo monomer **10** and endo monomer **11** cannot be resolved and appear as a common signal at δ = −7.83. In contrast, the endo,endo dimer **12** displays two ^{6}Li signals, which are assigned to the "sandwiched" lithium (δ = −12.45 ppm) and to the "external" THF-solvated lithium (δ = −0.98 ppm), as was found for isodiCpLi (**1**).

Introduced by our group,[9,10a-f] ^{6}Li, ^{1}H two-dimensional heteronuclear Overhauser effect spectroscopy (HOESY)[11] has now been employed extensively for the detection of short ^{6}Li-^{1}H distances.[9,10] In the case of isodiCpli (**1**),[4] HOESY confirmed the presence of an equilibrium between exo monomer **7** and exo,exo dimer **8**.

Figure 3 shows the ^{6}Li,^{1}H HOESY spectrum of CCpLi (**2**) in THF-d_8 at −107 °C. The HOESY pulse sequence[8] involves a mixing period, during which the heteronuclear NOE builds up. For the spectrum of Figure 3, a mixing time of 1.8 s was selected. During this period, rapid exchange takes place between the three aggregates, **10**, **11**, and **12**. Thus, the NOE is transferred to positions that were not originally involved in the NOE ("false" NOEs; cf. ref 8). Consequently, all f_1 cross sections taken at the chemical shifts of the three ^{6}Li peaks (Figure 3b–d) in principle contain cross peaks at identical ^{1}H chemical shifts. The discrepancies between the individual f_1 cross sections lie in the different signal-to-noise ratios that originate from different ^{6}Li peak heights.

Nonetheless, valuable information may be obtained from the HOESY spectrum of **2** in THF-d_8; cross peaks are observed at the ^{1}H chemical shifts of the Cp protons H3, H4 and H5. This shows Li^+ to be attached closely to the Cp moiety ("contact ion pair"). However, this does not differentiate between an exo or an endo location of lithium.

The aliphatic proton cross peak at $\delta_{^1H}$ = 1.68 ppm indicates that H8(endo) and H9(endo) are involved in the heteronuclear NOE. Hence, at least one species with an endo lithium location must be present. On the other hand, the cross peaks involving the syn methyl groups H13 indicate that at least one species with exo-located lithium is present in the equilibrium mixture. These results are in complete agreement with all the other NMR spectra.

As a further validation of the NMR assignments to **10**, **11**, and **12**, the integrals of the ^{6}Li NMR signals may be compared with the ^{1}H NMR integrals. In the ^{6}Li NMR spectrum of **2** in THF-d_8, the integral ratio between the peak at δ = −7.83 ppm and the peak at δ = −12.45 ppm is 3.9:1. This evidently represents the molar ratio of monomers to dimers. From the assignments of the ^{1}H

(10) (a) Bauer, W.; Müller, G.; Pi, R.; Schleyer, P. v. R. *Angew. Chem.* **1986**, *98*, 1130. *Angew. Chem., Int. Ed. Engl.* **1986**, *25*, 1103. (b) Bauer, W.; Klusener, P. A. A.; Harder, S.; Kanters, J. A.; Duisenberg, A. J. M.; Brandsma, L.; Schleyer, P. v. R. *Organometallics* **1988**, *7*, 552. (c) Gregory, K.; Bremer, M.; Bauer, W.; Schleyer, P. v. R. *Ibid.* **1990**, 9, 1485. (d) Hoffmann, D.; Bauer, W.; Schleyer, P. v. R. *Chem. Commun.* **1990**, 208. (e) Bauer, W.; Schleyer, P. v. R. In *Advances in Carbanion Chemistry*, Vol. 1; Snieckus, V., Ed.; Jai Press: Greenwich, CT; In press. (f) Bauer, W.; Schleyer, P. v. R. *Magn. Reson. Chem.* **1988**, *26*, 827. (g) Günther, H. *Proceedings of the 10th National Conference on Molecular Spectroscopy with International Participation*, Bulgarian Academy of Science, Blagdoevgrad, Bulgaria, 1988. (h) Harder, S.; Boersma, J.; Brandsma, L.; van Mier, G. P. M.; Kanters, J. A. *J. Organomet. Chem.* **1989**, *364*, 1. (i) Moene, W.; Vos, M.; de Kanter, F. J. J.; Klumpp, G. W.; Spek, A. L. *J. Am. Chem. Soc.* **1989**, *111*, 3463. (k) Arnett, E. M.; Fisher, F. J.; Nichols, M. A.; Ribeiro, A. A. *Ibid.* **1989**, *111*, 748. (l) Arnett, E. M.; Fisher, F. J.; Nichols, M. A.; Ribeiro, A. A. *Ibid.* **1990**, *112*, 801. (m) Harder, S.; Boersma, J.; Brandsma, L.; Kanters, J. A.; Duisenberg, A. J. M.; van Lenthe, J. H. *Organometallics* **1990**, *9*, 511.

(11) (a) Rinaldi, P. L. *J. Am. Chem. Soc.* **1983**, *105*, 5167. (b) Yu, C.; Levy, G. C. *Ibid.* **1983**, *105*, 6994. (c) Yu, C.; Levy, G. C. *Ibid.* **1984**, *106*, 6533.

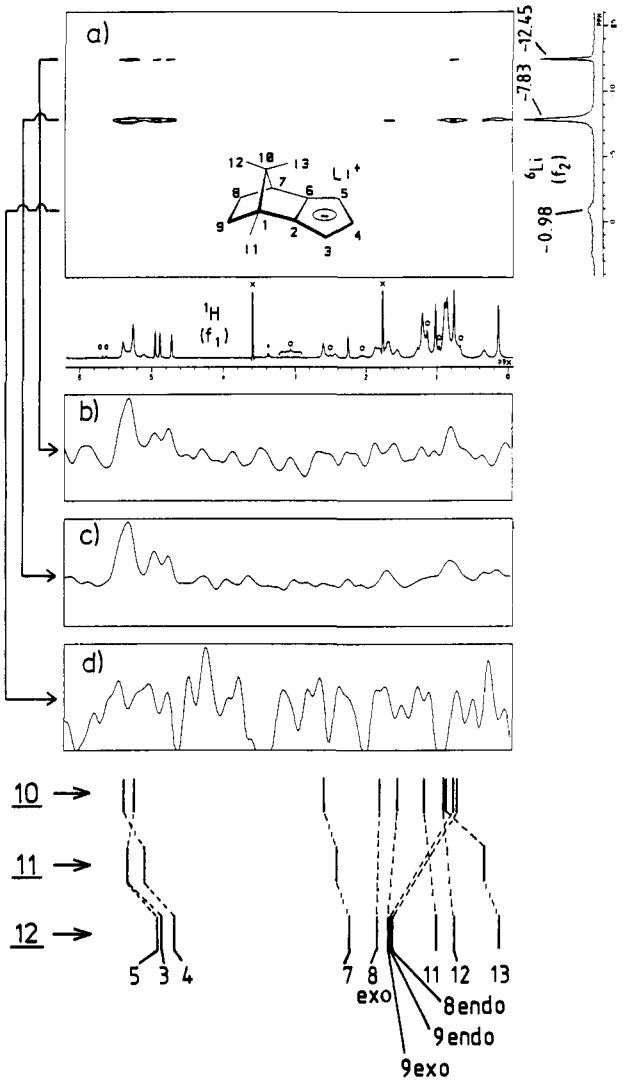

Figure 3. ^{6}Li,^{1}H HOESY spectrum of CCpLi **2** in THF-d_8, 0.34 M, −107 °C; mixing time 1.8 s; overall measuring time 24 h. (a) Contour plot. (b–d) f_1 cross sections taken at the chemical shifts of the three observed ^{6}Li signals. For the assignments of the ×, +, and ○ peaks, see Figure 1.

chemical shifts to the individual isomers given above, the molar ratio between the monomers (**10** + **11**) and the dimer **12** (as derived from the ^{1}H integrals) is 3.8:1. This agrees with the results obtained from the ^{6}Li integrals. Alternative interpretations of the ^{1}H NMR resonances (e.g. interchange of the assignments of endo monomer **11** and endo,endo dimer **12** or assuming that exo,exo dimer **17** is present instead of endo monomer **11**) result in a severe mismatch of the ^{6}Li and ^{1}H NMR integrals. Hence, the ternary equilibrium between **10**, **11**, and **12** is supported further.

In hydrocarbon solvents, Fraenkel[12] previously observed up to five coexisting aggregates of propyllithium (hexamers to nonamers). *Inter*aggregate exchange was found to be comparatively slow on the NMR time scale for these species under the experimental conditions.

Numerous examples of organolithium compounds have been described that involve binary equilibria in etheral solvents (THF, dimethoxyethane, diethyl ether), e.g. dimeric/tetrameric *n*-butyllithium[5a] or monomeric/dimeric phenyllithium.[9c] In contrast to the behavior in nonpolar solvents, interaggregate exchange is faster in these media.

To the best of our knowledge, no ternary equilibria have been observed hitherto for organoalithium compounds *in THF*. Thus, our observed mixture of exo monomer **10**, endo monomer **11**, and endo,endo dimer **12** represents a noteworthy situation where three organolithium species are observed at low temperatures in comparable amounts.

Equilibrium at Room Temperature. Time-averaged signals are found at 25 °C in the ^{1}H, ^{13}C, and ^{6}Li NMR spectra of **2**. Nonetheless, the relative ratio of the individual isomers may still be determined within certain limits of accuracy. We must assume that the ^{13}C chemical shifts of the three isomers are identical both at −107 °C and at 25 °C. Furthermore, we must preclude any further species at 25 °C that were not present at −107 °C.

Two of the ^{13}C chemical shifts of the isomers observed at −107 °C (Table II) show exceptionally large variations; the C10 values range from 56.85 ppm to 64.10 ppm, and C4 ranges from 95.09 to 100.84 ppm. In order to calculate the molar ratios, these chemical shifts are correlated with the averaged values obtained at 25 °C. In addition, the sums of the molar fractions are taken to be unity.

We can thus write the following equations:

$$56.85p_x + 64.10p_n + 64.02p_d = 59.55 \quad (1)$$

$$100.84p_x + 95.09p_n + 96.88p_d = 99.09 \quad (2)$$

$$p_x + p_n + p_d = 1.0 \quad (3)$$

Here, p denotes the molar fraction, and indices x, n, and d denote exo monomer **10**, endo monomer **11**, and endo, endo dimer **12**, respectively.

Solution of eqs 1–3 leads to $p_x = 0.62$, $p_n = 0.15$, and $p_d = 0.23$, which estimates the molar ratio of **10**, **11**, and **12** at room temperature. This result is nearly identical with the molar ratios deduced at −107 °C (see above). Thus, CCpLi seems to be an exceptional case where an (ternary) equilibrium is essentially independent of temperature. This behavior of CCpLi (**2**) contrasts with that of isodiCpLi (**1**). For the latter, the equilibrium of monomer **7** and dimer **8** observed at −100 °C was completely shifted towards exo monomer **7** at room temperature.[4]

We agree with a referee and emphasize that the above evaluation of the molar ratio of **10**, **11**, and **12** at room temperature is only a rather crude approach. These results are inherently not as accurate as those obtained at −107 °C.

MNDO Calculations. Semiempirical MNDO calculations[13] are established as a powerful tool in the structural analysis of organolithium compounds.[14] Despite the known deficiencies of the MNDO parametrizations for Li (e.g. overestimation of Li,C and Li,H interactions[15]), quite accurate relative energetic orderings often are obtained within one series of compounds. We have successfully applied MNDO for the prediction of second metalations in 1-naphthyllithium[9d] and for the interpretation of experimental results on the ortho lithiation of anisole.[9a] With isodiCpLi (**1**), MNDO calculations agreed favorably with the experimental NMR results.[4]

Figure 4 shows the MNDO structures of different monomers and dimers of CCpLi (**2**) as well as their heats of formation. The monomers were calculated with both exo and endo locations of lithium, as well as with different numbers of attached water ligands (used as models for THF). The exo isomers are always more stable

(12) Fraenkel, G.; Henrichs, M.; Hewitt, J. M.; Su, B. M.; Geckle, M. J. *J. Am. Chem. Soc.* **1980**, *102*, 3345.

(13) Dewar, M. J. S.; Thiel, W. *J. Am. Chem. Soc.* **1977**, *99*, 4899 and 4907. Li parametrization: Thiel, W.; Clark, T. Unpublished work.

(14) Bausch, J. W.; Gregory, P. S.; Olah, G. A.; Prakasch, G. K.; Schleyer, P. v. R.; Segal, G. A. *J. Am. Chem. Soc.* **1989**, *111*, 3633. McKee, M. L. *Ibid.* **1987**, *109*, 559. Hacker, R.; Kaufmann, E.; Schleyer, P. v. R.; Mahdi, W.; Dietrich, H. *Chem. Ber.* **1987**, *120*, 1533. Hacker. R.; Schleyer, P. v. R.; Reber, G.; Müller, G.; Brandsma, L. *J. Organomet. Chem.* **1986**, *316*, C4. Wilhelm, D.; Clark, T.; Schleyer, P. v. R.; Dietrich, H.; Mahdi, W. *J. Organomet. Chem.* **1985**, *280*, C6. Schleyer, P. v. R.; Hacker, R.; Dietrich, H.; Mahdi, W. *Chem. Commun.* **1985**, 622. Neugebauer, W.; Geiger, G. A. P.; Kos, A. J.; Stezowski, J. J.; Schleyer, P. v. R. *Chem. Ber.* **1985**, *118*, 1504. Stezowski, J. J.; Hoier, H.; Wilhelm, D.; Clark, T.; Schleyer, P. v. R. *Chem. Commun.* **1985**, 1263. Dietrich, H.; Mahdi, W.; Wilhelm, D.; Clark, T.; Schleyer, P. v. R. *Angew. Chem.* **1984**, *96*, 623. *Angew. Chem., Int. Ed. Engl.* **1984**, *23*, 621. Boche, G.; Decher, G.; Etzrodt, H.; Dietrich, H.; Mahdi, W.; Kos, A. J.; Schleyer, P. v. R. *Chem. Commun.* **1984**, 1493.

(15) Kaufmann, E.; Raghavachari, K.; Reed, A.; Schleyer, P. v. R. *Organometallics* **1988**, *7*, 1597.

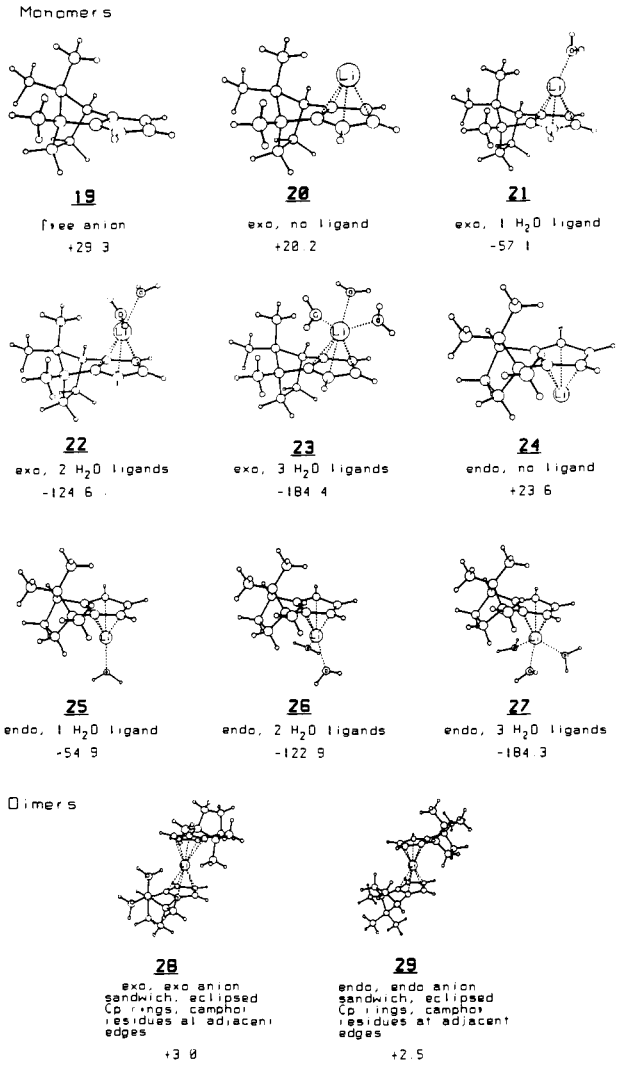

Figure 4. MNDO calculated structures of various stereoisomers, haptomers, and aggregates of CCpLi **2**. The heats of formation, $\Delta H_f°$, are given in kilocalories/mole. Water was used as a model for the donor ligand, THF. All structures were optimized by using the keyword PRECISE.

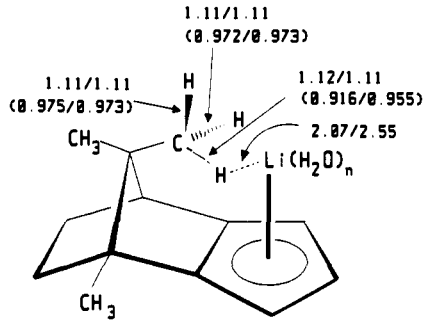

Figure 5. Li,H interaction in the MNDO calculated exo monomers **20** and **26** (cf. Figure 4). Values at bonds without brackets represent bond lengths in angstroms; values within brackets are bond orders. Values preceding the slashes refer to exo monomer **20**; values following the slashes refer to exo monomer **26**.

than the corresponding endo counterparts. At first glance, this seems unexpected because of the bulk of the syn methyl group C13. However, the exo preference in the monomers **20–27** apparently is due to favorable agostic interactions between lithium and the methyl hydrogen atoms. The proximity of lithium to nonbonded hydrogens is well-documented to be favorable.[15]

This preference is most obvious in the exo monomer with no ligand, **20**. As shown by the details in Figure 5, MNDO predicts an appreciable Li interaction with one of the H13 hydrogen atoms; the Li–H distance is quite short (2.07 Å), and the corresponding C–H bond order is considerably reduced. The same tendency, albeit weaker, is predicted by MNDO for the same exo monomer when three H_2O ligands are present (**26**, Figure 5).

Equations 4–11 summarize the MNDO energies (in kilocalories/mole) of the Li^+–cation–anion interactions and of the stepwise solvation of the monomers. The MNDO heats of formation of Li^+ and H_2O are +156.7 and −60.9 kcal/mol, respectively.

exo monomers

$$\underset{+29.3}{\mathbf{19}} + \underset{+156.7}{Li^+} \rightleftharpoons \underset{+20.2}{\mathbf{20}} \qquad \Delta H = -165.8 \tag{4}$$

$$\underset{+20.2}{\mathbf{20}} + \underset{-60.9}{H_2O} \rightleftharpoons \underset{-57.1}{\mathbf{21}} \qquad \Delta H = -16.4 \tag{5}$$

$$\underset{-57.1}{\mathbf{21}} + \underset{-60.9}{H_2O} \rightleftharpoons \underset{-124.6}{\mathbf{22}} \qquad \Delta H = -6.6 \tag{6}$$

$$\underset{-124.6}{\mathbf{22}} + \underset{-60.9}{H_2O} \rightleftharpoons \underset{-184.4}{\mathbf{23}} \qquad \Delta H = +1.1 \tag{7}$$

endo monomers

$$\underset{+29.3}{\mathbf{19}} + \underset{+156.7}{Li^+} \rightleftharpoons \underset{+23.6}{\mathbf{24}} \qquad \Delta H = -162.4 \tag{8}$$

$$\underset{+23.6}{\mathbf{24}} + \underset{-60.9}{H_2O} \rightleftharpoons \underset{-54.9}{\mathbf{25}} \qquad \Delta H = -17.6 \tag{9}$$

$$\underset{-54.9}{\mathbf{25}} + \underset{-60.9}{H_2O} \rightleftharpoons \underset{-122.9}{\mathbf{26}} \qquad \Delta H = -7.1 \tag{10}$$

$$\underset{-122.9}{\mathbf{26}} + \underset{-60.9}{H_2O} \rightleftharpoons \underset{-184.3}{\mathbf{27}} \qquad \Delta H = -0.5 \tag{11}$$

dimers

$$\underset{+29.3}{\mathbf{19}} + \underset{+23.6}{\mathbf{24}} \rightleftharpoons \underset{+2.5}{\mathbf{29}} \qquad \Delta H = -50.4 \tag{12}$$

$$\underset{+29.3}{\mathbf{19}} + \underset{+20.2}{\mathbf{20}} \rightleftharpoons \underset{+3.0}{\mathbf{28}} \qquad \Delta H = -46.5 \tag{13}$$

Equations 12 and 13 show the calculated energies for the endo,endo and the exo,exo dimer anion sandwiches. The endo,endo dimer is more favorable, in agreement with the NMR findings. In solution, the dimer anion (a triple ion) is associated with the $[Li(THF)_4]^+$ cation. This also might influence the relative stabilities.[4]

Mechanistic Aspects of Quenching Reactions. We have studied the reaction of CCpLi (**2**) with $TiCl_3$, $CpTiCl_3$, $ZrCl_4$, $ZrCpCl_3$, and $ZrCp''Cl_3$ ($Cp'' = C_5(CH_3)_5$).[3] In contrast to isodiCpLi (**1**),[2a] CCpLi (**2**) does not react with any of these electrophiles at low temperatures (−78 °C). Even at room or even more elevated temperatures, long reaction times (several hours to days) are required in order to obtain reasonable yields of the quenching products. Whereas at least some endo selectivity always is found, the endo:exo ratio ranges widely, extending from 13:1 to 1.4:1.[3]

We have proposed a mechanism for the quenching reactions of isodiCpLi (**1**) involving the lithium cation, which acts as a directing atom for the quenching reagent.[4] The reactions were assumed to proceed on the same side as the lithium. The switch from endo (−78 °C) to exo (25 °C) selectivity in quenching reactions of **1** was ascribed to reflect the molar ratio of the involved aggregates, **7** and **8**; at 25 °C, isodiCpLi (**1**) exists exclusively as exo monomer **7**.[4]

In contrast, CCpLi (**2**) exists as an equilibrium of exo monomer **10**, endo monomer **11**, and endo,endo dimer **12** in comparable amounts at 25 °C in THF. Reactions of exo monomer **10** and endo,endo dimer **12** might be expected to lead to exo quenching products. Even though endo quenching products are expected from reactions of endo monomer **11**, this species has the lowest concentration in THF at 25 °C (see above). Thus, the observed strong endo preference in quenching reactions of **2** implies that end monomer **11** must be the most reactive species. We attribute this to steric hindrance in the transition states. The bulky syn methyl group (C13) inhibits reactions at the exo face.

Conclusions

We have observed—perhaps for the first time—a *ternary* equilibrium of an organolithium compound in THF. CCpLi (**2**) exists as an exo monomer **10**, as an endo monomer **11**, and as an endo,endo dimer **12** in THF at −107 °C. For a 0.34 M solution, the molar ratio of **10**:**11**:**12** is 57:21:22. Approximately the same isomer composition is deduced from time-averaged ^{13}C chemical shifts to persist at room temperature. In the ^{6}Li NMR spectrum of CCpLi (**2**) magnetic anisotropy leads to unusual upfield chemical shifts. This was observed earlier for isodiCpLi (**1**).[4] Two-dimensional $^{6}Li,^{1}H$ HOESY confirms the location of lithium in the individual isomers.

Semiempirical MNDO calculations are in good agreement with the NMR results. The unexpected preference for the exo location of lithium in the monomer is indicated by MNDO to be due to favorable agostic Li–H interactions. These involve the protons of the syn methyl group of the methano bridge in **2**.

That endo quenching products are predominantly found in reactions of CCpLi (**2**) must be a consequence of steric hindrance. While species **10** and **12** of the organolithium reagent might lead to exo products, endo monomer **11** is assumed to be the most reactive species. This may be a consequence of the directing effect of lithium; attachment of the quenching reagent to lithium at the endo face might be preferred energetically in the reaction transition states.

Experimental Section

All experiments were performed in flame-dried glassware under an atmosphere of dry argon.

Synthesis of [(1*R*,7*S*)-1,10,10-Trimethyltricyclo[5.2.1.0^{2,6}]deca-2,5-dien-3-yl]lithium (2). From a solution of diene **9** in diethyl ether the solvent was removed in vacuo. The remaining procedure followed that described in ref 3 by using ^{6}Li-enriched *n*-butyllithium.[5a]

NMR spectra were recorded on a JEOL GX400 spectrometer (9.4 T; ^{1}H, 400 MHz). ^{1}H and ^{13}C NMR spectra are referenced to the signals of the deuterated solvent, THF-d_8: ^{1}H, residual α-H, δ = 3.58 ppm; ^{13}C, α-C, δ = 67.4 ppm. ^{6}Li spectra are referenced to 1 M LiBr in THF/THF-d_8. The reference measurements were carried out prior to the sample measurements at the indicated temperatures.

Spectral Parameters of 2D NMR Spectra.[6] **C,H Shift Correlation (Figure 1)**: A 0.34 M solution of THF-d_8, −107 °C. 90° pulse widths: 9 μs (^{13}C) and 15 μs (^{1}H). Spectral widths: 12723 Hz (^{13}C, f_2) and 2517 Hz (^{1}H, f_1). 4096 data points in t_2, zero filled to 8192 data points. 128 increments in t_1, 64 scans per t_1 increment, Gaussian window in t_1 and t_2. **ROESY (Figure 2)**: A 0.34 M solution in THF-d_8, −107 °C. 90° pulse width: 36 μs (attenuated). Spectral width: 2518 Hz. 1024 data points in t_2, 128 increments in t_1, zero filled to 256 data points. 32 sancs per t_1 increment. Spin lock time: 250 ms [repetitive sequence (12 μs pulse–120 μs delay)$_{320}$; cf. ref 16]. Exponential weighting in t_1 and t_2. **$^{6}Li,^{1}H$ HOESY (Figure 3)**: A 0.34 M solution in THF-d_8, −107 °C. 90° pulse widths: 23 μs (^{6}Li) and 26 μs (^{1}H). Spectral widths: 1200 Hz (^{6}Li, f_2) and 2518 Hz (^{1}H, f_1). 512 data points in f_2, 48 increments in t_1, zero filled to 256 data points. 64 scans per t_1 increments. Gaussian weighting in t_1 and t_2. Pure absorption quadrature detection in f_1.[17]

MNDO calculations were carried out on a CONVEX C210 computer by using the VAMP4 (vectorized AMPAC) software package.[18] All geometry optimizations involved the keyword PRECISE.[19]

Acknowledgment. We thank T. Clark for the vectorized AMPAC program (VAMP4). Financial support by the Deutsche Forschungsgemeinschaft, the Fonds der Chemischen Industrie, the Stiftung Volkswagenwerk, and the National Institutes of Health (Grant CA-12115) is gratefully acknowledged. G.A.O. thanks the U.S. Department of Education for a National Needs Fellowship.

(16) Kessler, H.; Griesinger, C.; Kerssebaum, R.; Wagner, K.; Ernst, R. R. *J. Am. Chem. Soc.* **1987**, *109*, 607.
(17) States, D. J.; Haberkorn, R. A.; Ruben, D. J. *J. Magn. Reson.* **1982**, *48*, 286.
(18) The Dewar Research Group and J. J. P. Stewart, Quantum Chemistry Program Exchange, No. 506, 1986.
(19) Clark, T. *A Handbook of Computational Chemistry*; Wiley: New York, 1985.

^{29}Si Magic-Angle-Spinning NMR Spectroscopy Quantitatively Monitors the Double-Chain/Triple-Chain Intergrowths in Hydrous Silicates

João Rocha,[†] Mark D. Welch,[‡] and Jacek Klinowski*,[†]

Contribution from the Department of Chemistry, University of Cambridge, Lensfield Road, Cambridge CB2 1EW, U.K., and the Department of Earth Sciences, University of Cambridge, Downing Street, Cambridge CB2 3EQ, U.K. *Received March 8, 1991*

Abstract: Stacking phenomena play a central role in the kinetics of many mineral transformations, and quantitative determination of stacking sequences is therefore of major importance. The application of equilibrium thermodynamics to petrological problems depends on the correct interpretation of the thermodynamic status of the various regular and disordered stacking variants. Determination of the proportions of different polysome sequences (e.g. the ratio of double-chain to triple-chain silicates in an intergrowth) is essential to any thermodynamic study of polytypic/polysomatic transformations and disequilibrium time–temperature–transformation studies, from which the cooling histories of metamorphic rocks can be deduced. Although crystal intergrowths can often be imaged by high-resolution transmission electron microscopy, the technique is not suitable for the quantitative determination of polysome proportions. We have examined a polysomatic intergrowth of sodium clinojimthompsonite (hydrous triple-chain structure) and a chemically equivalent sodic amphibole (hydrous double-chain structure) and report that ^{29}Si magic-angle-spinning (MAS) NMR spectroscopy enables the populations of double- and triple-chain silicates in fine-scale lamellar intergrowths of the two polymorphs to be quantitatively determined.

The biopyriboles[1-3] are a family of chain silicates of major petrological interest. The family includes the pyroxenes (single-chain), amphiboles (hydrous double-chain), hydrous triple-chain silicates, and micas (hydrous sheet structures). They form a polysomatic series with pyroxene and mica end-members, denoted by MTO_3 and $AM_3T_4O_{10}(OH)_2$, respectively (A = interlayer site in micas, M = 6- and 8-coordinated atoms, T = tetrahedral atoms). The polysomatic behavior of the series can be considered in terms of the stacking of pyroxene and mica to form

[†] Department of Chemistry.
[‡] Department of Earth Sciences.

(1) Veblen, D. R.; Buseck, P. R.; Burnham, C. W. *Science* **1977**, *198*, 359-365.
(2) Thompson, J. B. *Min. Soc. Am. Rev. Min.* **1981**, *9A*, 141–186.
(3) Veblen, D. R.; Burnham, C. W. *Am. Mineral.* **1978**, *63*, 1053–1073.

0002-7863/91/1513-7100$02.50/0